THE JOURNAL OF BIOLOGICAL CHEMISTRY VOL. 286, NO. 8, pp. 6650–6658, February 25, 2011

Targeted *in Vivo O*-GlcNAc Sensors Reveal Discrete Compartment-specific Dynamics during Signal Transduction*[S]

Received for publication, October 5, 2010, and in revised form, November 29, 2010 Published, JBC Papers in Press, December 7, 2010, DOI 10.1074/jbc.M110.191627

Luz D. Carrillo[‡], **Joshua A. Froemming**[‡], **and Lara K. Mahal**[‡§1]

From the [‡]*Department of Chemistry and Biochemistry, University of Texas, Austin, Texas 78712 and the* [§]*Department of Chemistry, New York University, New York, New York 10003*

β-*O*-*N*-acetyl-D-glucosamine (*O*-GlcNAc) is a post-translational modification involved in a plethora of biological systems ranging from cellular stress to insulin signaling. This modification shares many hallmarks with phosphorylation, including its dynamic cycling onto a host of proteins such as transcription factors, kinases, and phosphatases, and regulation of cellular functions, including cell signaling. Herein, we report the development of an improved genetically based *O*-GlcNAc FRET sensor and compartmentalized targeted variants for the characterization of the spatiotemporal dynamics of *O*-GlcNAc. During serum-stimulated signal transduction, rapid increases in *O*-GlcNAc activity were observed at both the plasma membrane and the nucleus, with a concomitant decrease detected in the cytoplasm. These findings suggest the existence of compartment specific dynamics for *O*-GlcNAc in response to signal-inducing stimuli, pointing to complex regulation of this modification. In addition, inhibition of the PI3K pathway by wortmannin abolished the *O*-GlcNAc response, suggesting that the activity observed is modulated downstream of the PI3K pathway. Taken together, our data argues that *O*-GlcNAc is a rapidly induced component of signaling and that the interplay between *O*-GlcNAc and kinase signaling may be more akin to the complex relationship between kinase pathways.

Dynamic post-translational events coordinate the ability of cells to respond to changes in their microenvironment. The post-translational modification β-O-*N*-acetyl-D-glucosamine (*O*-GlcNAc) is emerging as a key regulator of cellular activities through the modulation of signal transduction. Recent findings have shown a role for this modification in the attenuation of insulin signaling, cellular stress response, and aging (1–3). *O*-GlcNAc modifies a diversity of proteins including those involved in signaling and gene regulation. These include kinases (*e.g.* Akt1), phosphatases, and transcription factors such as STAT5, c-Myc, Sp1, and p53 (4–7). The effects of *O*-GlcNAc, like phosphorylation, are substrate-specific and can include alteration of the subcellular locale, stability of proteins, and modulation of protein-protein interactions (8–10). The interplay between phosphorylation and *O*-GlcNAc in signal transduction is not well understood (11). On some substrates, *O*-GlcNAcylation directly impacts the phosphorylation status of the protein through either direct or indirect competition. There is also evidence that *O*-GlcNAc can alter the activity of kinases (12, 13). *O*-GlcNAc transferase (OGT)[2] itself may be regulated by kinases, as tyrosine phosphorylation of this enzyme has been associated with higher levels of OGT activity (14). *O*-GlcNAc levels are thought to be sensitive to alterations in glucose, which change the levels of UDP-GlcNAc, the critical sugar donor for the modification. Glucose metabolism, therefore, has been advocated as one mechanism for the control of this modification (8). Perturbations in *O*-GlcNAcylation have been linked to several disease states including type II diabetes and Alzheimer disease (15).

O-GlcNAc cycles onto cytoplasmic and nuclear serine/threonine sites through the actions of only two enzymes. A unique glycosyltransferase OGT adds the GlcNAc moiety, whereas its removal is mediated via a specific β-*O*-N-acetylglucosamidase (*O*-GlcNAcase). Although only a single gene exists for each enzyme, both are known to have several splice variants. *O*-GlcNAcase has two splice variants, a full-length version, whose localization is mainly cytosolic, and a catalytically less active nuclear-localized variant that is missing a putative histone acetyltransferase domain (16). For OGT, three variants have been identified, short- and full-length nuclear/cytoplasmic localized versions and a mitochondrial localized enzyme (17). These variants differ in their N termini but are identical throughout their C-terminal catalytic domains, which contain a unique phosphoinositide-binding domain. Serum stimulation of Cos7 cells activates PI3K, which synthesizes the phosphoinositide PIP3, causing OGT to be rapidly recruited to the plasma membrane through this domain. Insulin stimulation of adipocytes also results in the dynamic compartmentalization of OGT, arguing that the relocalization of this enzyme may be a general mechanism to control *O*-GlcNAc activity during signal transduction (1, 14). However, concomitant changes in compartment specific

* Financial Support for this work came from the American Heart Association (Grant-in-aid, 0755146Y) and the Alfred P. Sloan Foundation.

[S] The on-line version of this article (available at http://www.jbc.org) contains supplemental "Methods," Figs. S1–S8, and Movies 1–9.

[1] To whom correspondence should be addressed: 100 Washington Square East, Rm. 1001, New York, NY 10003. Fax: 212-995-4475; E-mail: lkmahal@nyu.edu.

[2] The abbreviations used are: OGT, *O*-GlcNAc transferase, also known as UDP-GlcNAc:polypeptide *O*-GlcNAc transferase; PIP3, inositol 1,4,5-trisphosphate; OS, *O*-GlcNAc sensor; CFP, cyan fluorescent protein; HBSS, Hank's balanced salt solution; *O*-GlcNAcase, β-*O*-*N*-acetyl-glucosamidase; *O*-GlcNAcylation, modification of Ser/Thr by *O*-GlcNAc; PUGNAc, 2-acetamido-2-deoxy-D-glucopyranosylidene amino-*N*-phenylcarbamate.

O-GlcNAc activity were not documented in these studies (1). In general, the spatiotemporal dynamics of *O*-GlcNAc upon signaling have not been examined.

Our laboratory created the first genetically encoded FRET-based sensor, to monitor the dynamics of the *O*-GlcNAc modification in living cells (18). The *O*-GlcNAc sensor (OS) is composed of a FRET pair, enhanced cyan fluorescent protein, and the yellow fluorescent protein variant Venus, a β-*O*-GlcNAc-specific fimbrial lectin from *Escherichia coli* (GafD), and a known *O*-GlcNAc substrate peptide from casein kinase II. Upon *O*-GlcNAcylation of the substrate domain, intramolecular recognition of the GlcNAc moiety by GafD changes the distance of the two fluorophores leading to an increase in FRET between enhanced cyan fluorescent protein and Venus. *In vitro* studies demonstrated that the *O*-GlcNAc-modified substrate is accessed by the *O*-GlcNAcase enzyme, reversing the FRET signal and allowing for visualization of *O*-GlcNAc dynamics. Under conditions of increasing *O*-GlcNAc levels, this sensor was able to monitor the activity of *O*-GlcNAc enzymes in live cells (18).

Herein, we report the development of an improved *O*-GlcNAc reporter and compartment-targeted variants for the characterization of the spatiotemporal dynamics of *O*-GlcNAc in serum-stimulated signal transduction. Our data argues for complex regulation of *O*-GlcNAc within a signaling cascade. Rapid increases in *O*-GlcNAc are observed at both the plasma membrane and the nucleus in response to serum. In contrast, a decrease in *O*-GlcNAc activity is seen in the cytoplasm. These findings suggest the existence of compartment specific dynamics for *O*-GlcNAc in response to serum stimulation, arguing a role for localization in the regulation of this modification. In addition, we observe direct inhibition of the *O*-GlcNAc response with wortmannin treatment, suggesting that this response is modulated downstream of the PI3K pathway. The use of our compartmentalized sensors in tandem with known stimuli and inhibitors is beginning to illuminate the complex spatiotemporal regulation of *O*-GlcNAc.

EXPERIMENTAL PROCEDURES

Gene Construction of Improved Sensor and Its Targeted Variants—The improved *O*-GlcNAc sensor (OS2) was composed of an enhanced cyan fluorescent protein (CFP) fused to the fimbrial adhesin lectin domain GafD (19, 20), a known substrate peptide domain for *O*-GlcNAc from casein kinase II placed between two flexible linkers (GGSGG) followed by a variant of the yellow fluorescent protein Venus. The control sensors created had an active GafD domain, but all of the serine or threonine residues in the casein kinase II domain were changed to alanines or glycines.

The nuclear localization sequence from SV40, PKKRKVEDA (21), was attached to the construct OS2 at the C terminus to create the construct Nuc-OS2. The cytoplasmic sensor Cyto-OS2 was generated by tethering the nuclear exclusion sequence from HIV-1 Rev protein, LPPLERLTL (22), to the C terminus of the OS2 construct. Fusion of the myristoylation and palmitoylation sequence, GCINSKRK (23) from Lyn kinase to the N terminus of the OS2 construct, targeted the PM-OS2 sensor and its control (PM-OS2 control) to the plasma membrane. All inserts encoding each FRET-based sensor gene were initially created in prSET A and subcloned into mammalian expression vector pCDNA3.1(−) A His/Myc (Invitrogen) using restriction sites BamHI and HindIII. The detailed cloning strategies and primers can be found in the supplemental Methods. The inserts and vectors were gel purified using the QIAquick Gel Extraction kit (Qiagen) and ligated using T4 DNA ligase (New England Biolabs). The sensors were transformed into DH5α *E. coli* cells and plated on selective media. A 100-ml culture of each of the constructs transformed into *E. coli* DH5α cells was grown to saturation and plasmids were purified using a QIAprep Endo-free Kit (Qiagen).

Cell Culture and Transfection—Both HeLa and Cos7 cells were used in our experiments, HeLa for the initial testing of the improved sensor OS2 and localized sensors with PUGNAc/glucosamine and Cos7 for all serum data. HeLa cells were maintained in Eagle's minimum essential medium (1 g/liter glucose (low glucose)) supplemented with nonessential amino acids and sodium pyruvate (HyClone) containing 10% fetal bovine serum at 37 °C in 5% CO_2. Cos7 cells were maintained in high glucose Dulbecco's modified Eagle's medium (HyClone, 4.5 g/liter) containing 10% fetal bovine serum at 37 °C in 5% CO_2. Cells were plated at 60% confluency onto sterile 35 × 10 mm glass-bottomed plates (InVitro Scientific) prior to transfection of the appropriate plasmid using FuGENE 6 reagent (Roche Applied Science). After 10–12 h of transfection, the cells were serum-starved for 16–20 h prior to imaging experiments. During serum starvation, the cells were incubated in 0.1% fetal bovine serum in their corresponding media.

Cell Imaging—Cells were washed and maintained in Hank's balanced salt solution (HBSS) at 37 °C for each of the imaging experiments. The amount of glucose in HBSS was kept constant (*i.e.* 1 g/liter for HeLa and 4.5 g/liter for Cos7 cells). HeLa cells were stimulated with 100 μM PUGNAc and 4 mM glucosamine as described previously (18). Cos7 cells were stimulated with serum. Cells were imaged prior to and immediately following the addition of stimuli ($t = 0$, stimuli addition). Images were acquired on a TE2000-U inverted microscope (Nikon Instruments Inc.) using a Sony Cool Snap ES 1300 × 1030 camera controlled by MetaMorph software. All optical filters were obtained from Chroma Technologies. CFP and FRET images were obtained either every 2 min (HeLa PUGNAc, $GlcNH_2$ experiments) or every 30 s (all Cos7 experiments) through an S430/25× filter, a 86022v2bs dichroic mirror, and two emission filters (S470/30m and S535/30m), respectively. A YFP image was obtained as a control through S500/20× excitation filter, a 86022v2bs dichroic mirror, and a S535/30m emission filter. Excitation and emission filters were switched via filter wheels (Lambda 10-3, Sutter). Exposure times for CFP and FRET were 100–200 ms and 50 ms for YFP. Fluorescence images were background corrected and then thresholded. The ratiometric FRET image, which is shown in all figures, was calculated by dividing the back-

ground subtracted and thresholded FRET image by the background-subtracted CFP image.

The resulting ratiometric FRET images were reanalyzed using MetaMorph software. Only cells with an average intensity of half of a 12-bit image in YFP were selected. After addition of stimuli, changes in the average intensity of YFP between the first and second frame did not allow us to include the initial time of the experiment ($t = 0$) in the calculation of the FRET response. Our data presents a 30 s–2 min delay for each experiment. Regions were selected in the YFP channel image and then transferred to the ratiometric FRET image. Analysis of the OS2 sensor consisted of the selection of a region in the nucleus and the cytoplasm for each cell. In the case of the Nuc-OS2 sensor, a region that encompassed the whole nucleus was selected. Linear regions that contained no net cell movement over time were selected to examine the Cyto-OS2 and PM-OS2 sensors. The resulting FRET ratio values were normalized to 1 by dividing all of the time point values by the value of the starting point.

Statistical Analysis—*p* values were obtained by a paired Student's *t* test (two-tailed) analysis of the normalized average FRET ratios of the OS2 and its control sensor after 30 min of serum treatment. Nuclear and cytoplasmic normalized average FRET ratios of seven cells for each sensor were examined. The GraphPad QuickCalcs Software was utilized to perform the calculations.

RESULTS

Creation of a Second Generation O-GlcNAc Sensor with Improved Dynamic Range—We created a second generation *O*-GlcNAc sensor (OS2) by altering the region containing the linker and substrate domains. Previous work by Allen and Zhang (24) demonstrated that variations to the length of the linker region could affect the FRET response of sensors. The OS2 sensor incorporates two shorter linker regions, one on each side of the substrate domain, in lieu of the single linker region between the GafD and the substrate in the original *O*-GlcNAc sensor (Fig. 1*A*) (18). On average, the change in FRET values observed for the OS2 reporter were 2-fold higher than those seen for the original sensor when subjected to our test conditions, *i.e.* HeLa cells treated with 100 μM PUGNAc and 4 mM glucosamine (15–30% for OS2 compared with 7–15% for OS, Fig. 1*B*). The OS2 sensor has a higher dynamic range, which in turn improves the signal-to-noise ratio, increasing probe sensitivity and allowing the analysis of more subtle changes in the dynamics. A matched control sensor for OS2 (OS2 control, Fig. 1*A*) containing no serines or threonines in the substrate domain was also created. As expected, this sensor showed no significant FRET changes under the test conditions (supplemental Fig. 1). Given the enhancement in dynamic range, the OS2 sensor was used as the template for creating a series of compartmentally targeted *O*-GlcNAc sensors.

Creation of Compartmentally Targeted O-GlcNAc Sensors—Signal transduction goes through a series of precisely localized and timed post-translational modifications, the most studied of which has been phosphorylation (25). Targeting of *in vivo* FRET sensors for phosphorylation to specific cellular

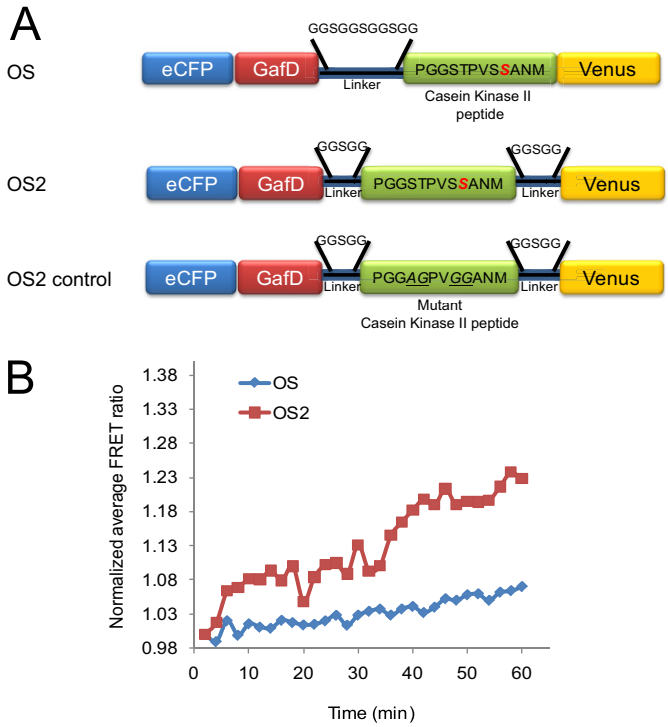

FIGURE 1. **Characterization and comparison of the *O*-GlcNAc FRET-based sensors OS and OS2.** *A*, schematic of the *O*-GlcNAc reporters OS, OS2, and OS2 control. The *O*-GlcNAc sensors were composed of an enhanced CFP (*eCFP*) fused to the fimbrial adhesin lectin domain GafD (19, 20), a known substrate peptide domain for *O*-GlcNAc from casein kinase II and a variant of the yellow fluorescent protein; Venus. The OS2 sensor incorporates two shorter linker regions, one on each side of the substrate domain, in lieu of the single linker region between the GafD and the substrate in the original *O*-GlcNAc sensor, OS. The OS2 control sensor does not contain serine or threonine residues in the casein kinase II substrate domain. *B*, HeLa cells were transfected with OS and OS2 and ratiometric FRET measurements were quantified for 60 min immediately following the addition of PUGNAc (100 μM) and glucosamine (4 mM). The OS2 sensor displays a higher dynamic range than the OS sensor. The graph is representative of the three independent experiments.

compartments has allowed more defined interrogation of kinase/phosphatase dynamics (24, 26). Although *O*-GlcNAc is thought to play a role in signaling, the localization and dynamics of the *O*-GlcNAc response in signal transduction has not been characterized. To facilitate our exploration of the spatiotemporal dynamics of *O*-GlcNAc in signaling, we created a series of *O*-GlcNAc sensors targeted to the nucleus, cytoplasm and plasma membrane (Fig. 2*A*). We generated the nuclear-localized OS2 sensor (Nuc-OS2) by fusing the C terminus of OS2 with a nuclear localization sequence derived from SV40 (supplemental Fig. 2) (27). The cytoplasm-localized sensor (Cyto-OS2) was generated by fusion of a nuclear exclusion peptide from the HIV-1 Rev protein to the C terminus of OS2 (28). Testing of Nuc-OS2 and Cyto-OS2 under our standard conditions (HeLa cells, 100 μM PUGNAc, 4 mM glucosamine) showed the expected compartment-specific increases in FRET (supplemental Fig. 3). To create our plasma membrane sensor (PM-OS2), we fused a peptide sequence from Lyn kinase containing both a myristoylation and palmitoylation site to the N terminus of our sensor (23). This sequence targets proteins to lipid raft domains at the cell surface (29). A matched control sensor targeted to the plasma

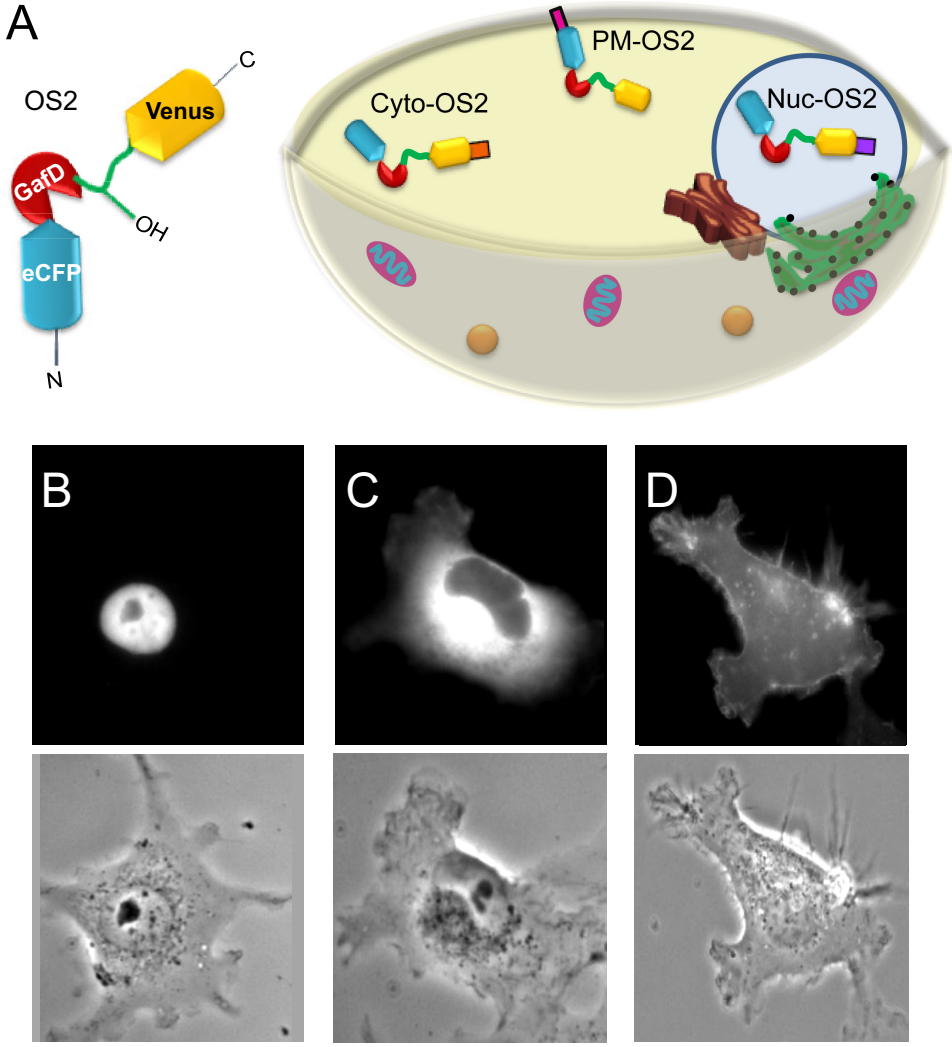

FIGURE 2. **Compartmentalization of the OS2 reporter.** *A*, schematic representation of the targeted OS2 sensors. *B*, the nuclear-localized OS2 sensor (*Nuc-OS2*) was created by fusing the C terminus of OS2 with a nuclear localization sequence derived from the simian virus 40 large T-antigen. *C*, Cyto-OS2 was generated by fusion of a nuclear exclusion peptide from the HIV-1 Rev protein to the C terminus of OS2. *D*, the plasma membrane sensor (PM-OS2) contains a peptide sequence from Lyn kinase with both a myristoylation and palmitoylation site fused to the N terminus of the OS2 sensor. *eCFP*, enhanced CFP.

membrane (PM-OS2 control) was also generated. The subcellular localization of our targeted sensors was verified by fluorescence microscopy (Fig. 2, *B–D*), with additional verification of the locale of the plasma membrane sensor via confocal microscopy (supplemental Fig. 4).

O-GlcNAc Displays Differential Dynamics in Nucleus and Cytoplasm during Serum Response—Serum contains a high amount of growth factors and has been utilized to study a variety of mitogenic signaling pathways, including the PI3K pathway (30–32). Fibroblasts deficient in *O*-GlcNAc fail to upregulate early serum response transcription factors such as c-Fos, c-Jun, and c-Myc, arguing a role for *O*-GlcNAc signaling in serum response (33). To gain an overall view of the dynamics of the *O*-GlcNAc modification during serum-induced signal transduction, we utilized the nontargeted OS2 sensor. In brief, serum-starved Cos7 cells transiently transfected with the OS2 sensor were stimulated with serum and imaged using fluorescence microscopy (supplemental Movie 1). Although a small but significant increase in FRET was observed in the nucleus ($3.3 \pm 1.13\%$, $n = 7$, $p < 0.0001$ paired Student's *t* test, compared with control sensor), on average, the cytoplasm showed little change during the same 30-min time frame, although a decrease in the FRET ratio was observed in some cells ($-1.2 \pm 2.6\%$, $n = 7$, $p = 0.1457$, Fig. 3*A*). The OS2 control sensor showed no change in FRET in either compartment upon treatment with serum (Fig. 3*B*). As expected, in the absence of serum stimulation no changes in the FRET ratio were observed in the cell (supplemental Fig. 5 and supplemental Movie 2).

To further dissect the discrete dynamics of *O*-GlcNAc within the cell, we utilized our nuclear and cytoplasm-localized sensors (Nuc-OS2 and Cyto-OS2, respectively). Compartmentalization of the sensors improved their dynamic range. Data obtained with the localized sensors corroborated our previous observations and confirmed a decrease in FRET in the cytoplasm upon serum stimulation (Fig. 4 and supplemental Movies 3 and 4). Activation of *O*-GlcNAc in the nucleus was rapid, starting within a minute after addition of sera. Under our imaging conditions, we accumulated data 30 s after the addition of stimuli and observed a response by the

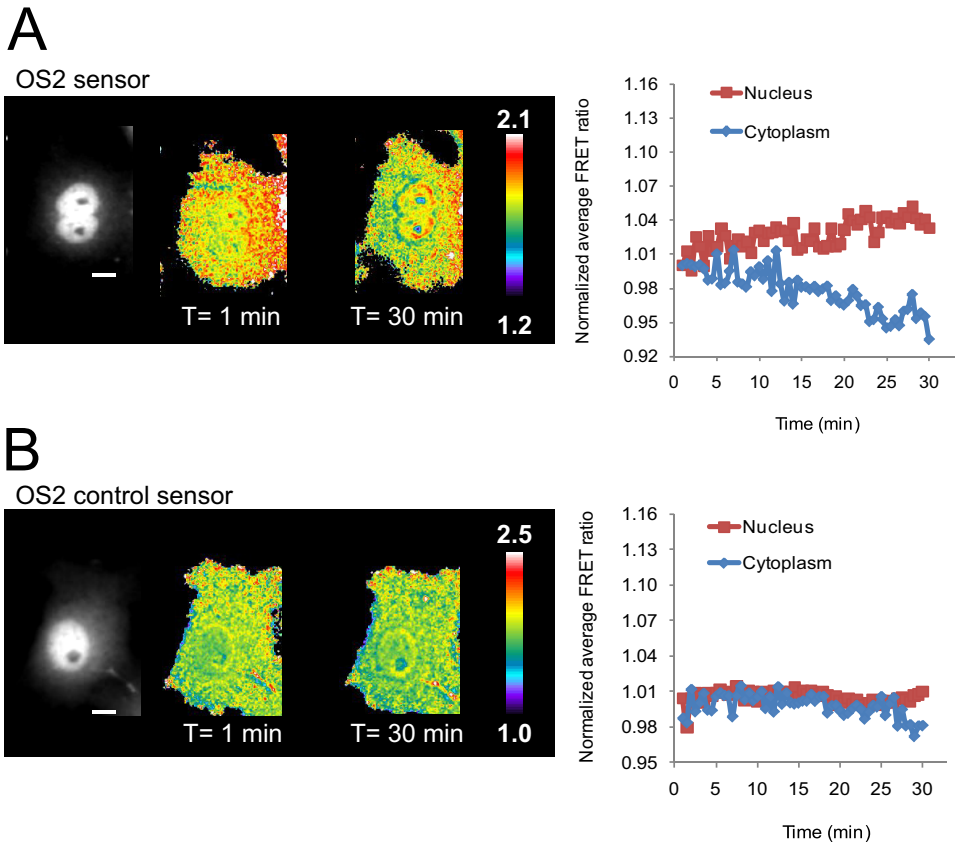

FIGURE 3. ***O*-GlcNAc response during serum stimulation in Cos7 cells.** Cos7 cells expressing OS2 or OS2 control sensor were serum starved (16–20 h) and placed in imaging media (HBSS). Upon treatment with serum (10% FBS in HBSS), cells were monitored for 30 min (supplemental Movies 1 and 2, respectively). The monochrome image represents the YFP channel and shows the distribution of the reporter in the cell. *A*, FRET response of Cos7 cells transfected with the OS2 sensor. Pseudocolor images depict an increase in FRET in the nucleus and a slight decrease in the cytoplasm. The normalized average FRET ratio for this cell was plotted in a time course. The *scale bar* represents 30 μm. The *color bar* represents the FRET ratio values. *B*, FRET response of the OS2 control sensor. No change in FRET can be observed in either compartment upon treatment with serum. The graph on the *right* represents the normalized average FRET ratio for this cell over time. Data is representative of ~5–7 cells.

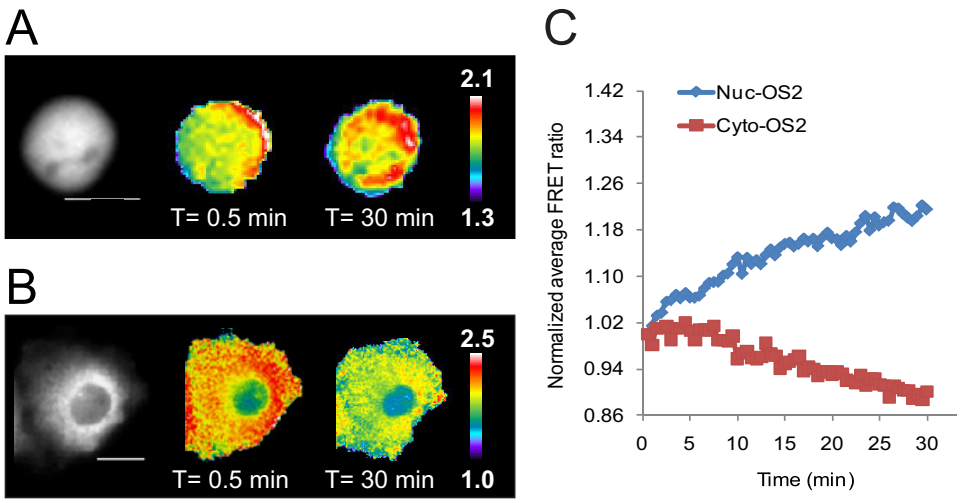

FIGURE 4. **Visualization of nuclear and cytoplasm-specific *O*-GlcNAc activity in Cos7 cells upon serum stimulation.** Cos7 cells expressing Nuc-OS2 or Cyto-OS2 sensor were treated as in Fig. 3 and imaged for 30 min after serum stimulation (supplemental Movies 3 and 4, respectively). The *far left* image represents the YFP channel monochrome image. *A*, Cos7 cells transfected with the Nuc-OS2 sensor displayed an increase in FRET over the 30-min time frame. *B*, Cos7 cells transfected with the Cyto-OS2 sensor showed a clear decrease in FRET over time. The *scale bar* represents 20 μm for both the Nuc-OS2 sensor (*A*) and Cyto-OS2 (*B*) sensors. The *color bar* represents the FRET ratio values. *C*, graph of the normalized average FRET ratio over time for cells shown in *A* and *B*. Nuc-OS2 data is shown in *blue*, and the Cyto-OS2 data is visualized in *red*. Data are representative for a minimum of three cells from independent experiments.

first time point (*i.e.* 1 min). On average, the FRET response in the nucleus began to plateau at ~22 min reaching 11 ± 5.3% (n = 9) in a 30-min time frame (supplemental Fig. 6). In contrast, the data obtained with the cytoplasmic sensor shows a clear depletion of *O*-GlcNAc activity upon serum stimulation (Fig. 4, *B* and *C*, supplemental Fig. 7). Unlike the rapid re-

sponse in the nucleus, *O*-GlcNAc activity observed in the cytoplasm did not begin to decrease until ~8 min after the addition of serum and did not level off in the 30 min timeframe (−8.9 ± 1.2%, $n = 3$, t = 30 min). These findings provide the first evidence for compartment specific *O*-GlcNAc dynamics during signal transduction.

Local Regions of O-GlcNAc Activity Are Observed in Plasma Membrane upon Serum Stimulation—Serum-induced signal transduction initiates at the plasma membrane where recruitment of a myriad of proteins is induced by the transformation of PIP2 to PIP3 through PI3K activation. Recent work by Yang *et al.* (1) demonstrated that OGT, the enzyme that catalyzes *O*-GlcNAc transfer, is rapidly recruited to the plasma membrane through its interactions with phosphoinositides, most strongly PIP3, upon serum stimulation. Although the OGT-GFP construct utilized in their studies enabled visualization of OGT relocalization to the plasma membrane in Cos7 cells, concomitant changes in the activity of the enzyme were not described. To this end, we examined the dynamics of serum-stimulated *O*-GlcNAc signaling with our plasma membrane localized sensor (PM-OS2). In brief, serum-starved Cos7 cells transiently transfected with either PM-OS2 or PM-OS2-control were treated with serum and monitored using fluorescence microscopy. Upon serum stimulation, increases in FRET were observed in a minute within localized regions of the plasma membrane (*red arrow*, Fig. 5 and supplemental Movie 5). These regions are distributed at the edges of the cells, reminiscent of factors localized to membrane ruffles (34). This is in stark contrast to the even distribution of OGT-GFP recruited to the membrane observed by Yang *et al.* (1). Examination of several domains within different cells revealed that the signal begins to plateau at ~12 min (42 ± 23%, n = five domains from three cells, supplemental Fig. 8). No changes in FRET were observed anywhere along the plasma membrane for serum-stimulated cells transfected with our control sensor (PM-OS2-control, Fig. 5 and supplemental Movie 6). Our findings suggest that although OGT may be recruited to the entire plasma membrane, *O*-GlcNAc activity at the membrane upon serum stimuli is more localized, pointing to additional control mechanisms for this modification.

O-GlcNAc Response to Serum Requires Activation of PI3K Pathway—As a first step to understanding the interplay between the kinase pathways and *O*-GlcNAc signaling, we examined whether inhibition of the PI3K pathway would alter *O*-GlcNAc activity. For these experiments we utilized wortmannin, a well characterized inhibitor of this pathway, which inhibits the PIP3-dependent recruitment of OGT to the plasma membrane (1). Pretreatment of Cos7 cells with wortmannin (for 30 min at 100 nM) completely abolished the serum stimulated *O*-GlcNAc response in all three compartments (Fig. 6 and supplemental Movies 7–9). In addition, no alteration in the FRET signal was observed during wortmannin treatment in the absence of serum, consistent with what is seen in the absence of stimuli. This data argues that the PI3 kinase pathway is critical to *O*-GlcNAc signaling in response to serum and that PI3K and/or its downstream targets are responsible for the modulation of *O*-GlcNAc.

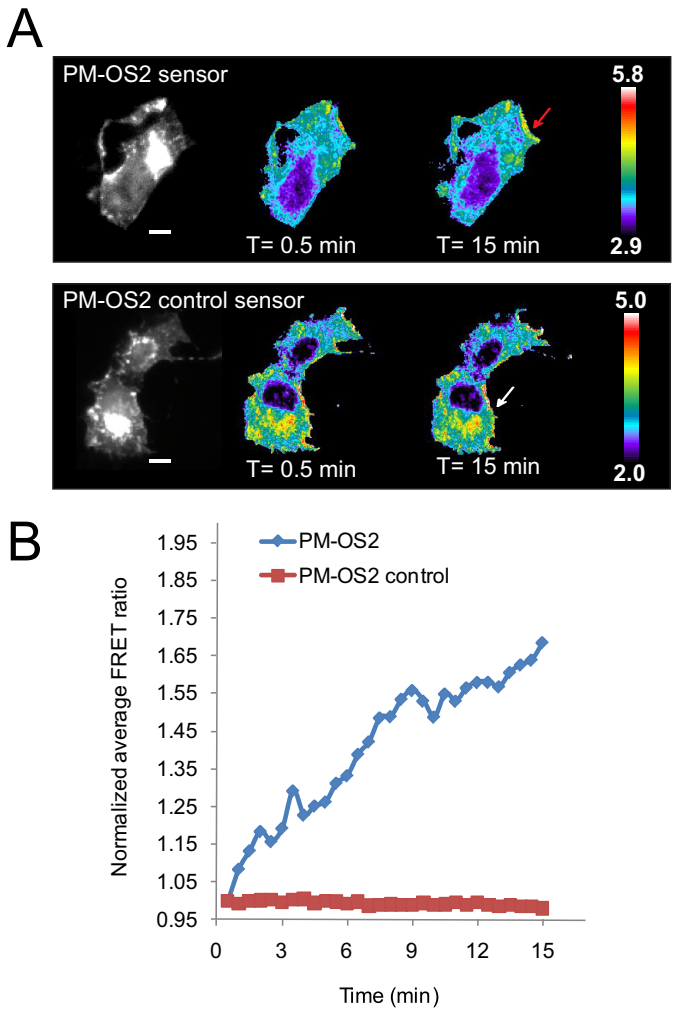

FIGURE 5. **Plasma membrane targeted OS2 sensor reveals localized microdomains of *O*-GlcNAc activity.** Serum-starved Cos7 cells transfected with either PM-OS2 or PM-OS2-control were treated with serum as before and their corresponding FRET changes were quantified (supplemental Movies 5 and 6, respectively). The regions utilized for the analysis of the FRET changes are labeled with *arrows*. *A*, upon serum stimulation, increases in FRET were observed within localized regions of the plasma membrane (*red arrow*). Overall, no change was observed in the plasma membrane of cells overexpressing the PM-OS2 control sensor (*white arrow*). The *scale bar* represents 30 μm for both PM-OS2 and PM-OS2 control sensors. The *color bar* represents the FRET ratio values. *B*, graphical representation of *A*. Data shown are representative of a minimum of three cells from independent experiments.

DISCUSSION

There is mounting evidence that *O*-GlcNAc is a component of signal transduction networks, with roles in a variety of cellular processes including insulin signaling, the cell cycle, and stress response (10). This modification shares similarities with phosphorylation, for example both dynamically cycle onto cytosolic and nuclear proteins, are inducible by a variety of external stimuli and can control protein function and stability (8, 35). In known kinase cascades, localization and timing of enzyme activity within the cell are critical components of the signal (36–39). These factors play an important role in determining the appropriate response to a given stimuli. Like many kinases, the enzymes responsible for *O*-GlcNAc cycling exist in both the cytoplasmic and nuclear compartments and OGT can be recruited to the plasma membrane. Protein/protein

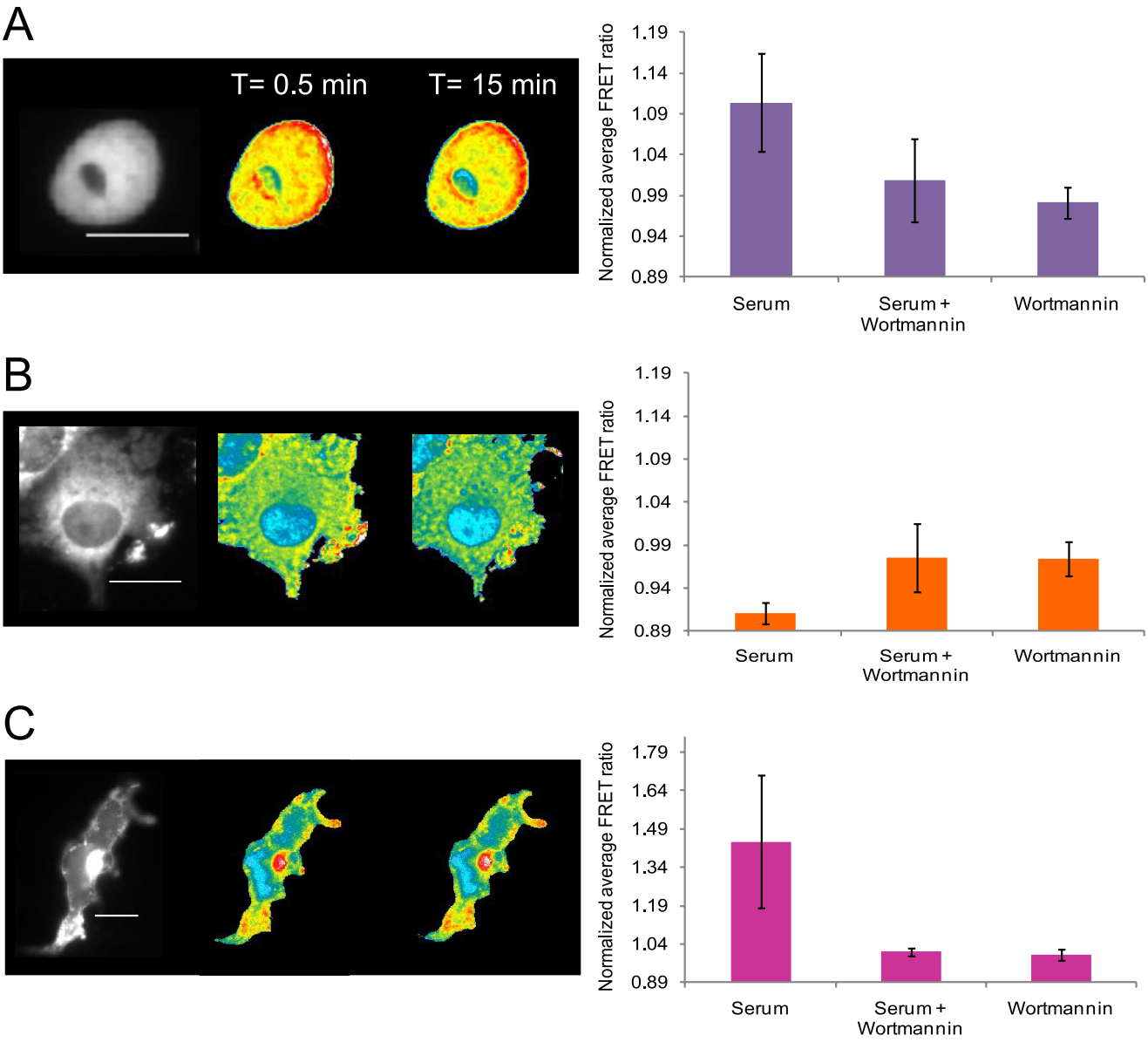

FIGURE 6. **Inhibition of the PI3K pathway by wortmannin abolishes *O*-GlcNAc dynamics in response to serum.** Serum-starved Cos7 cells transfected with the either the nuclear, the cytoplasmic, or the plasma membrane targeted OS2 sensors were pretreated with wortmannin (100 nM) for 30 min followed by stimulation with serum as before (supplemental Movies 7, 8, and 9, respectively). The YFP channel image (*far left*) shows the distribution of the reporter in the cell. Changes in FRET response for serum-starved Cos7 cells treated with wortmannin and serum are illustrated by pseudocolor images. The *color bar* represents the FRET ratio values. The *scale bar* represents 20 μm for all sensors. The bar graphs at the *right* of the FRET images represent the average FRET response of the sensors for a select number of cells treated with either serum, serum and wortmannin, or wortmannin alone. *A*, Nuc-OS2 data. The bar graph at the *right* represents the average data of seven cells with the S.D. for each treatment condition. *B*, Cyto-OS2 data. The bar graph at the *right* represents the average data of three cells with the S.D. for each treatment condition. *C*, PM-OS2 data. The bar graph at the *right* represents the average data of three cells with the S.D. for each treatment condition.

interactions, post-translational modifications, and the concentration of the sugar donor, UDP-GlcNAc, can also affect their activity, potentially modulating them in a location-dependent manner (11). Thus, localization and timing might play an important role in the *O*-GlcNAc component of signaling.

To examine whether *O*-GlcNAc showed spatially discrete dynamics in response to stimuli, we created a series of *O*-GlcNAc sensors targeted to the nuclear, cytoplasmic, and plasma membrane compartments, based on an improved variant of our original *in vivo* FRET sensor (OS2, Figs. 1 and 2). These sensors were then used to examine *O*-GlcNAcylation during serum-induced signaling. Our sensors revealed distinct localized dynamics for *O*-GlcNAc in response to serum. Rapid increases were observed in the nucleus and at localized portions of the plasma membrane, whereas a decrease in *O*-GlcNAc activity was detected in the cytoplasm.

One theory for how *O*-GlcNAc is controlled is that the concentration of the sugar donor UDP-GlcNAc regulates OGT activity (8). This ties *O*-GlcNAc to glucose metabolism as UDP-GlcNAc is a downstream product via the hexosamine biosynthetic pathway. Glucose converts to UDP-GlcNAc with a $t_{1/2} \sim 15$ min (44). If influx of glucose is the main mechanism

triggering *O*-GlcNAc in response to a signal, such as sera, we would expect a general increase over the whole cell in *O*-GlcNAc activity, as is observed when cells are treated with glucosamine and PUGNAc (Fig. 1). Our studies disagree with this as we see differential compartmentalized responses to sera on a faster time scale ($\leq$1 min) than would be accounted for by this mechanism. Hexosamine biosynthesis probably still plays a role in signal transduction by *O*-GlcNAc, but we suspect that the alterations in the levels of UDP-GlcNAc may alter the duration and strength of the signal, due to changes in basal level occupation of *O*-GlcNAc sites, rather than directly cause rapid changes in *O*-GlcNAc during signaling.

Preincubation of the cells with wortmannin, an inhibitor of the PI3K pathway abolished the serum-induced *O*-GlcNAc response in all compartments. This is consistent with evidence showing wortmannin inhibits *O*-GlcNAc-associated increases in neutrophil migration (40) and argues that PI3K plays an important role in regulation of the *O*-GlcNAc response. Several possibilities exist for how *O*-GlcNAc could be regulated by the PI3K pathway. Work by Yang *et al.* (1) argues that PI3K, through the creation of PIP3, directly controls *O*-GlcNAc activity through OGT relocalization, recruiting it from the nucleus and cytoplasm to the plasma membrane. In this work, the majority of nuclear OGT redistributed uniformly on the plasma membrane within 30 min of serum stimulation in Cos7 cells. If local OGT concentration were the only factor effecting *O*-GlcNAc activity, we would expect to observe a slow but steady decrease in nuclear and cytoplasmic FRET as well as an increase of activity over the entire plasma membrane. Our data points to a more complicated scenario. Although we observe a steady decline in cytoplasmic *O*-GlcNAc activity, consistent with the removal of OGT disrupting the balance between the transferase and the *O*-GlcNAcase; a rapid rise in activity is visualized in the nucleus with no depletion in *O*-GlcNAc levels observed at the 30-min time frame (Fig. 4). In addition, we observe discrete patches of *O*-GlcNAc activity at the plasma membrane in response to serum, in contrast to the previously observed uniform distribution (Fig. 5). It should be noted that our sensor is examining the activity of native OGT, whereas the relocalization work was done with an overexpressed OGT-GFP fusion, which might effect its distribution. Also, the Lyn kinase-based targeting domain on PM-OS2, though targeting the plasma membrane, is known to localize sensors to lipid raft domains at the cell surface (29). However, we do not observe a correlation between the concentration of the sensor and FRET activity (Fig. 5, compare YFP channel with FRET), which argues that the localized FRET activity is due to other factors. Taken together, our data argues that the control mechanisms for *O*-GlcNAc are more complex than simple dynamic recruitment of OGT to sites of activity.

Recent work by Hart and co-workers (14) has implicated tyrosine phosphorylation of OGT as a factor in modulating the enzyme. They showed that OGT is tyrosine-phosphorylated in response to insulin and that phosphorylation enhances enzyme activity. OGT is a substrate for multiple tyrosine kinases, including the activated insulin receptor and Src kinase (14). OGT contains 15 potential Src kinase phosphorylation sites. Interestingly, activated Src kinase is localized to sites of membrane ruffling in Cos7 cells, where it plays a role in EGF receptor activation, one of the many pathways stimulated by serum (41). Our plasma membrane sensor shows highly localized *O*-GlcNAc activity at the edges of the membrane in response to serum stimulation (Fig. 5). This pattern is reminiscent of membrane ruffling and may be due to a combination of plasma membrane recruitment of OGT by PIP3 and more highly localized activation of the enzyme by a secondary factor such as a tyrosine kinase. This would be consistent with both the localization and wortmannin inhibition data. Src family kinases are also localized in the nucleus, potentially providing an explanation for the rapid stimulation of *O*-GlcNAc observed in this compartment (42). It is unclear in this case how the PI3K pathway would be involved.

Alternatively, other downstream effectors of the PI3K pathway may modulate OGT in a localized manner. OGT is known to modify Akt, a well characterized downstream kinase. Additionally, inhibition of GSK3β, another downstream kinase, alters the *O*-GlcNAcylation patterns observed in Cos7 cells (43). However, neither OGT nor *O*-GlcNAcase are presently known to be directly modified by these kinases.

The potentially complex mechanisms by which *O*-GlcNAc is controlled via kinase pathways and vice versa is a subject for further study. Overall, our data is painting a picture of *O*-GlcNAc as an integrated component of signal transduction. In contrast to the previous view of *O*-GlcNAc as a mass regulator of kinase signaling via interference with phosphorylation, either through direct or indirect competition, the rapid and localized kinetics of *O*-GlcNAc regulation argue that *O*-GlcNAc is a reponse element of signaling in its own right. Thus, the interplay between *O*-GlcNAc and kinase signaling may be more akin to the complex relationship between kinase pathways.

REFERENCES

1. Yang, X., Ongusaha, P. P., Miles, P. D., Havstad, J. C., Zhang, F., So, W. V., Kudlow, J. E., Michell, R. H., Olefsky, J. M., Field, S. J., and Evans, R. M. (2008) *Nature* **451,** 964–969
2. Whelan, S. A., Dias, W. B., Thiruneelakantapillai, L., Lane, M. D., and Hart, G. W. (2010) *J. Biol. Chem.* **285,** 5204–5211
3. Love, D. C., Ghosh, S., Mondoux, M. A., Fukushige, T., Wang, P., Wilson, M. A., Iser, W. B., Wolkow, C. A., Krause, M. W., and Hanover, J. A. (2010) *Proc. Natl. Acad. Sci. U.S.A.* **107,** 7413–7418
4. Nanashima, N., Asano, J., Hayakari, M., Nakamura, T., Nakano, H., Yamada, T., Shimizu, T., Akita, M., Fan, Y., and Tsuchida, S. (2005) *J. Biol. Chem.* **280,** 43010–43016
5. Yang, X., Su, K., Roos, M. D., Chang, Q., Paterson, A. J., and Kudlow, J. E. (2001) *Proc. Natl. Acad. Sci. U.S.A.* **98,** 6611–6616
6. Chou, T. Y., Hart, G. W., and Dang, C. V. (1995) *J. Biol. Chem.* **270,** 18961–18965
7. Yang, W. H., Kim, J. E., Nam, H. W., Ju, J. W., Kim, H. S., Kim, Y. S., and Cho, J. W. (2006) *Nat. Cell Biol.* **8,** 1074–1083
8. Zachara, N. E., and Hart, G. W. (2006) *Biochim. Biophys. Acta.* **1761,** 599–617
9. Hanover, J. A., Krause, M. W., and Love, D. C. (2010) *Biochim. Biophys. Acta* **1800,** 80–95
10. Butkinaree, C., Park, K., and Hart, G. W. (2010) *Biochim. Biophys. Acta.* **1800,** 96–106
11. Zeidan, Q., and Hart, G. W. (2010) *J. Cell Sci.* **123,** 13–22
12. Gandy, J. C., Rountree, A. E., and Bijur, G. N. (2006) *FEBS Lett.* **580,** 3051–3058

13. Park, S. Y., Ryu, J., and Lee, W. (2005) *Exp. Mol. Med.* **37,** 220–229
14. Whelan, S. A., Lane, M. D., and Hart, G. W. (2008) *J. Biol. Chem.* **283,** 21411–21417
15. Dias, W. B., and Hart, G. W. (2007) *Mol. Biosyst.* **3,** 766–772
16. Macauley, M. S., Whitworth, G. E., Debowski, A. W., Chin, D., and Vocadlo, D. J. (2005) *J. Biol. Chem.* **280,** 25313–25322
17. Love, D. C., Kochan, J., Cathey, R. L., Shin, S. H., Hanover, J. A., and Kochran, J. (2003) *J. Cell Sci.* **116,** 647–654
18. Carrillo, L. D., Krishnamoorthy, L., and Mahal, L. K. (2006) *J Am. Chem. Soc.* **128,** 14768–14769
19. Saarela, S., Taira, S., Nurmiaho-Lassila, E. L., Makkonen, A., and Rhen, M. (1995) *J Bacteriol.* **177,** 1477–1484
20. Tanskanen, J., Saarela, S., Tankka, S., Kalkkinen, N., Rhen, M., Korhonen, T. K., and Westerlund-Wikström, B. (2001) *J Bacteriol.* **183,** 512–519
21. Makkerh, J. P., Dingwall, C., and Laskey, R. A. (1996) *Curr. Biol.* **6,** 1025–1027
22. Fischer, U., Huber, J., Boelens, W. C., Mattaj, I. W., and Lührmann, R. (1995) *Cell* **82,** 475–483
23. Zacharias, D. A., Violin, J. D., Newton, A. C., and Tsien, R. Y. (2002) *Science* **296,** 913–916
24. Allen, M. D., and Zhang, J. (2006) *Biochem. Biophys. Res. Commun.* **348,** 716–721
25. Walsh, C. T., Garneau-Tsodikova, S., and Gatto, G. J., Jr. (2005) *Angew. Chem. Int. Ed. Engl.* **44,** 7342–7372
26. Gallegos, L. L., Kunkel, M. T., and Newton, A. C. (2006) *J. Biol. Chem.* **281,** 30947–30956
27. Wen, W., Meinkoth, J. L., Tsien, R. Y., and Taylor, S. S. (1995) *Cell* **82,** 463–473
28. Ullman, K. S., Powers, M. A., and Forbes, D. J. (1997) *Cell* **90,** 967–970
29. Gao, X., and Zhang, J. (2008) *Mol. Biol. Cell* **19,** 4366–4373
30. Raught, B., Gingras, A. C., Gygi, S. P., Imataka, H., Morino, S., Gradi, A., Aebersold, R., and Sonenberg, N. (2000) *EMBO J.* **19,** 434–444
31. Gonzalez, F. A., Seth, A., Raden, D. L., Bowman, D. S., Fay, F. S., and Davis, R. J. (1993) *J. Cell Biol.* **122,** 1089–1101
32. Tigyi, G., Dyer, D., Matute, C., and Miledi, R. (1990) *Proc. Natl. Acad. Sci. U.S.A.* **87,** 1521–1525
33. O'Donnell, N., Zachara, N. E., Hart, G. W., and Marth, J. D. (2004) *Mol. Cell. Biol.* **24,** 1680–1690
34. Saxena, A., Morozov, P., Frank, D., Musalo, R., Lemmon, M. A., Skolnik, E. Y., and Tycko, B. (2002) *J. Biol. Chem.* **277,** 49935–49944
35. Zachara, N. E., and Hart, G. W. (2002) *Chem. Rev.* **102,** 431–438
36. Zhang, J., Campbell, R. E., Ting, A. Y., and Tsien, R. Y. (2002) *Nat. Rev. Mol. Cell Biol.* **3,** 906–918
37. Violin, J. D., Zhang, J., Tsien, R. Y., and Newton, A. C. (2003) *J. Cell Biol.* **161,** 899–909
38. Kholodenko, B. N., Hancock, J. F., and Kolch, W. (2010) *Nat. Rev. Mol. Cell Biol.* **11,** 414–426
39. Alaimo, P. J., Shogren-Knaak, M. A., and Shokat, K. M. (2001) *Curr. Opin. Chem. Biol.* **5,** 360–367
40. Kneass, Z. T., and Marchase, R. B. (2005) *J. Biol. Chem.* **280,** 14579–14585
41. Donepudi, M., and Resh, M. D. (2008) *Cell Signal* **20,** 1359–1367
42. Takahashi, A., Obata, Y., Fukumoto, Y., Nakayama, Y., Kasahara, K., Kuga, T., Higashiyama, Y., Saito, T., Yokoyama, K. K., and Yamaguchi, N. (2009) *Exp. Cell Res.* **315,** 1117–1141
43. Wang, Z., Pandey, A., and Hart, G. W. (2007) *Mol. Cell Proteomics* **6,** 1365–1379
44. Marshall, S., Nadeau, O., and Yamasaki, K. (2004) *J. Biol. Chem.* **279,** 35313–35319